Original Article

Extracellular vesicles delivering nuclear factor I/C for hard tissue engineering: Treatment of apical periodontitis and dentin regeneration

Journal of Tissue Engineering
Volume 13: 1–18

DOI: 10.1177/20417314221084095
journals.sagepub.com/home/tej
SAGE

Shengyan Yang[1,2*], Qing Liu[1,2*], Shijing Chen[1,2*], Fuping Zhang[2,3], Yaoyin Li[2,4*], Wenguo Fan[2*], Lijia Mai[1,2*], Hongwen He[2,3] and Fang Huang[1,2*]

Abstract

Apical periodontitis (AP) causes arrest of tooth root development, which is associated with impaired odontoblastic differentiation of stem cells from apical papilla (SCAPs), but the underlying mechanism remains unclear. Here, we investigated roles of extracellular vesicle (EV) in AP and odontoblastic differentiation of SCAPs, moreover, a novel nuclear factor I/C (NFIC)-encapsulated EV was developed to promote dentin regeneration. We detected a higher expression of EV marker CD63 in inflamed apical papilla, and found that EVs from LPS-stimulated dental pulp cells suppressed odontoblastic differentiation of SCAPs through downregulating NFIC. Furthermore, we successfully constructed the NFIC-encapsulated EV by overexpressing NFIC in HEK293FT cells, which could upregulate cellular NFIC level in SCAPs, promoting the proliferation and migration of SCAPs, as well as dentinogenesis both in vitro and in vivo. Collectively, based on pathological roles of EV in AP, our study provides a novel strategy for dentin regeneration by exploiting EV to deliver NFIC.

Keywords

Extracellular vesicles, dentin regeneration, nuclear factor I/C, delivering transcription factor, apical periodontitis, stem cell from apical papilla

Date received: 6 December 2021; accepted: 13 February 2022

Introduction

Apical periodontitis (AP) is one of the most prevalent global dental diseases, characterized by inflammation and destruction of periapical tissues.[1,2] The occurrence of AP in the permanent but immature tooth represents a clinical challenge since it often causes arrest of tooth root development.[2] It's now considered that whether or not tooth root continue to develop largely depends on the regenerative activity of stem cells from apical papilla (SCAPs). SCAPs are a novel population of MSCs residing in the apical papilla of immature permanent teeth, which are the natural source of primary odontoblasts and critical for tooth root formation and maturation. Meanwhile, SCAPs are also regarded as promising stem cell candidates for pulp repair, dentin regeneration as well as bio-root engineering.[3,4] However, the biological activity of SCAPs in periapical inflammatory microenvironment remains largely elusive.

[1]Guanghua School of Stomatology, Hospital of Stomatology, Sun Yat-sen University, Guangzhou, China
[2]Department of Oral Anatomy and Physiology, Guanghua School of Stomatology, Hospital of Stomatology, Sun Yat-sen University, Guangzhou, China
[3]Guangdong Provincial Key Laboratory of Stomatology, Guangzhou, China
[4]Department of Pediatric Dentistry, Guanghua School of Stomatology, Hospital of Stomatology, Sun Yat-sen University, Guangzhou, China

*This author is now affiliated to Guangdong Provincial Key Laboratory of Stomatology, Guangzhou, China.

Corresponding authors:
Fang Huang, Guanghua School of Stomatology, Hospital of Stomatology, Sun Yat-sen University, 49 Huaxia Road, Guangzhou 510623, China.
Email: hfang@mail.sysu.edu.cn

Hongwen He, Guanghua School of Stomatology, Hospital of Stomatology, Sun Yat-sen University, 56 Lingyuan Xi Road, Guangzhou 510055, China.
Email: hehw@mail.sysu.edu.cn

Extracellular vesicles (EVs) are membranous vesicles that are secreted by most cell types,[5] and have been implicated in pathogenesis of various inflammation-related diseases,[6] including inflammatory bowel disease,[7] rheumatoid arthritis,[8] HIV infection,[9] and pneumonia.[10] EVs are also involved in inflammatory diseases within oral cavity, such as periodontitis, oral lichen planus, dental caries, and dental pulp infection.[11] It was recently reported that EV from LPS-stimulated odontoblasts protected neighboring odontoblasts from apoptosis during the progression of dental caries,[12] and EV from LPS-preconditioned dental pulp stem cells (DPSCs) and dental follicle cells (DFCs) promoted proliferation, migration, and differentiation of bone mesenchymal stem cells (BMSCs), Schwann cells, and periodontal ligament cells.[13–15] However, whether EVs are involved in pathophysiology of AP and the effect of EVs derived from dental pulp cells (DPCs) on odontoblastic differentiation of SCAPs remain largely unknown.

Given that EVs regulate a wide range of physiological processes and diseases, EV-based application is now a promising strategy for tissue repair and engineering, including dentin and other hard tissues regeneration.[11,16] EVs carry a variety of cargoes, including RNAs, proteins, lipids, and DNA, which can be taken up by local or distant target cells and execute defined biological functions.[17] EVs are now promising drug delivery vehicles owing to their intrinsic tissue-homing capabilities and ability to evade immune recognition and shield payload from chemical and enzymatic degradations.[18,19] EV-containing RNA cargo have become well-defined over the past decade and substantial advances have been made in therapeutic delivery of RNA via EVs, however, applicational efforts to deliver transcription factors are rarely explored. Nuclear factor I/C (NFIC) is a master transcription factor that's critical for odontogenesis and osteogenesis, and deficiency of NFIC contributes to short root anomaly (SRA) and dentin malformation. In this study, based on our finding that impaired odontoblastic differentiation is associated with a decline of NFIC in SCAPs, we attempted to transfer and replenish NFIC by exploiting EVs, hopefully, providing a novel strategy for AP therapy and hard tissue engineering.

In this research, we hypothesized that EV involves in pathophysiology of AP and detected the expression of EV surface marker CD63 in inflamed apical papilla of AP model. Moreover, we examined the effect of EV derived from LPS-stimulated dental pulp cells (LPS-EV) on odontoblastic differentiation of SCAPs and explored its putative mechanism by focusing on NFIC, which is a critical transcription factor for tooth root development. Most importantly, in view of the well-defined roles of NFIC in odontogenesis, we considered delivering NFIC via EV as a therapeutic method and developed the NFIC-encapsulated EV (NFIC-EV), next, we tested the effects of NFIC-EV on proliferation, migration of SCAPs, and dentinogenesis both in vitro and in vivo to validate its application potentials in dentin regeneration.

Materials and methods

Rat model of apical periodontitis in immature permanent teeth

The animal experiments were approved by the Ethics Committee of Sun Yat-sen University (Document No. 2021001248). Briefly, 5-week-old Sprague-Dawley rats were anesthetized by intraperitoneally injecting 2% pentobarbital sodium. To expose the pulp chamber at the pulp horn, upper portion of mandibular incisor was horizontally removed with round tungsten steel burs, and the entrance at pulp horn was enlarged with K-files #40 to create space for injecting lipopolysaccharide (LPS) dilution.[20] Five microliters of LPS from Escherichia coli O111:B4 (10 mg/mL, Sigma, USA) diluted in αMEM (Gibco, Grand Island, NY, USA) was injected onto exposed pulp tissue. As for control group, no treatments were performed. Animals were housed with food and water in a 12 h-light-dark cycle and were sacrificed after 21 days. The rats were anaesthetized with Thiopental (0.2 mL/100 g body weight) and sacrificed by exsanguination ($n = 3$ each group).

Cell culture

Rat dental pulp cells (DPCs) and stem cells from apical papilla (SCAPs) were primarily cultured from dental pulp and apical papilla tissues of 5-week-old SD rats, which were obtained from Laboratory Animal Center of Sun Yat-sen University (Guangzhou, China). After intraperitoneal anesthesia with 2% pentobarbital sodium, mandible incisors were separated and washed with phosphate-buffered saline (PBS, Gibco, Grand Island, NY, USA). Incisor pulp and apical papilla tissues were harvested and minced as previous described,[21,22] then seeded onto 10 cm^2 culture dishes with αMEM containing 20% fetal bovine serum (FBS; Gibco, Grand Island, NY, USA), 2% penicillin-streptomycin (Gibco, Grand Island, NY, USA) and 1% Gluta-Max (Gibco, Grand Island, NY, USA), subsequently expanded at 37°C with 5% CO_2. HEK293FT cells were cultured in high-glucose Dulbecco's modified Eagle medium (DMEM; Gibco, Grand Island, NY, USA) containing 10% fetal bovine serum (FBS) and 1% penicillin/streptomycin under 37°C and 5% CO_2. DPCs, SCAPs, and HEK293FT cells were passaged at 80% confluence with medium changed every 2–3 days. DPCs and SCAPs at passage 3–5 were used in following experiments.

Identification of DPCs and SCAPs

In colony formation assay, DPCs and SCAPs were seeded onto 10 cm^2 culture dishes at a low density (100 cells/plate)

and cultured for 7 days. After staining with 0.1% crystal violet for 30 min, colonies were observed in light scope. For immunocytochemistry of vimentin and cytokeratin, DPCs and SCAPs were fixed in 4% paraformaldehyde (Bioshrap, Anhui, China), permeabilized with 0.1% Triton X-100 (Sigma-Aldrich, USA), and blocked with 5% bovine serum albumin (BSA, BioFroxx, Germany). Cells were then incubated overnight with primary antibody: anti-cytokeratin antibody (1:100 dilution; Boster Bio, Hubei, China) and anti-vimentin antibody (1:100 dilution; Boster Bio, Hubei, China) and thereafter secondary antibody: DyLight® 488 goat anti-mouse IgG (1:200, EarthOx, CA, USA). Images were captured with LSM780 laser confocal scanning microscope (Zeiss, Oberkochen, Germany).

To identify osteogenic and adipogenic differentiation capability, DPCs and SCAPs were cultured with osteogenic induction medium (Cyagen, Guangzhou, China) or adipogenic induction medium (Cyagen, Guangzhou, China) when cells reached 80% confluence. After induction for 21 days, cells were fixed with 4% paraformaldehyde and stained with Alizarin Red staining solution (Cyagen, Guangzhou, China) or Oil Red O staining solution (Cyagen, Guangzhou, China). Images were captured with Fluorescence Inversion Microscope System (Carl Zeiss, Oberkochen, Germany).

The phenotype of DPCs and SCAPs were identified by flow cytometry. DPCs and SCAPs at third passage were resuspended as single cell suspensions and incubated with anti-CD29-FITC, anti-CD34-FITC, anti-CD44H-Alexa Fluor 647, anti-CD45-PE, and anti-CD90-PE antibodies (Biolegend, San Diego, CA, USA) in the dark. IgG1-FITC, IgG1-PE, and IgG1-AF647 were used as isotype controls and subsequently analyzed by flow cytometer (Beckman Coulter, CA, USA).

Isolation and identification of extracellular vesicle (EV)

EVs were isolated from culture medium of DPCs with or without treatment of LPS (0.1, 1, 10 μg/mL) for 3 days. Collected culture medium was centrifuged as previously published protocols[23]: 300 g for 10 min, 2000 g for 10 min, and 10,000 g for 30 min to eliminate cells and debris, followed by ultracentrifugation at 110,000 g for 70 min (Optima L-90 K; Beckman Coulter, USA). After washed once with PBS and centrifugation at 110,000 g for 70 min, supernatant was carefully removed and the pellet was resuspended in PBS. Besides, fetal bovine serum was ultracentrifuged at 100,000 g for 12 h to prepare EV-free serum, which was utilized for subsequent cell culture. Particle size distribution of collected EVs was identified by nanoparticle tracking analysis (NTA) (NanoSight NS300, Malvern, UK). After loaded onto a copper grid and stained with 2% (w/v) phosphotungstic acid for 5 min, EV morphology was examined by transmission electron microscopy (TEM; Japan). Protein concentration of EVs was quantified with a BCA Protein Assay Kit (Kangwei, Beijin, China), and the EV surface markers CD9 (1:1000, DF6565, Affinity Biosciences, USA), CD63 (1:1000, DF2305, Affinity Biosciences, USA), CD81(1:1000, Zen, Chendu, China), and TSG101 (1:1000, ab125011, Abcam, UK) were analyzed by western blot analysis.

Fluorescent labeling of EV and immunofluorescent staining

PKH26 (Umibio, Shanghai, China) was diluted in Diluent C and incubated with EVs for labeling and tracing EVs. After sequentially centrifuged as mentioned above, PKH26-labeled EVs were added to SCAPs and incubated for 48 h, cells were fixed with 4% paraformaldehyde and stained with Actin-Tracker Green-488 (Beyotime, Shanghai, China) for visualizing F-actin and 4′,6-diamidino-2-phenylindole (DAPI) for cell nucleus. The endocytosis of EVs by SCAPs was observed by confocal microscopy (Zeiss, Oberkochen, Germany).

Cell proliferation assay

DPCs (1×10^3 cells/well) were cultured in 96-well plates for 12 h and then cultured in αMEM containing 10% FBS with or without LPS (0.1, 1, 10 μg/mL) for 1, 3, 5, and 7 days. SCAPs (1×10^3 cells/well) were cultured in 96-well plates for 12 h and then cultured in αMEM containing 10% FBS with or without Nor-EV (10 μg/mL), four type LPS-EV (10 μg/mL), NFIC-EV (20 μg/mL), NC-EV (20 μg/mL) for 1, 3, 5, and 7 days. Cell proliferation was evaluated by Cell Counting Kit-8 assay (CCK-8, Dojindo, Japan).

Cell cycle assay

Cell cycle distribution of SCAPs was detected by Cell Cycle Detection Kit (KeyGen BioTech, Jiangsu, China). SCAPs that were treated with NFIC-EV (20 μg/mL) or NC-EV (20 μg/mL) for 3 days were resuspended as single cell suspensions and fixed with 70% cold ethanol overnight. After washing, cells were incubated with Propidium Iodide (PI)/RNase A for 30 min in dark, and subsequently analyzed by flow cytometry (Beckman Coulter, CA, USA). Statistics were analyzed with FlowJo software (BD Biosciences, USA).

Cell migration assay

Wound-healing and Transwell migration assays were employed to assess the migration of SCAPs after EVs treatment. For wound-healing assay, SCAPs (2×10^5 cells/well) were cultured in 6-well plates for 24 h. When cells reached 90% confluence, a wound scratch was created

with a sterile pipette tip, and culture medium was converted into FBS-free αMEM with or without EVs (20 μg/mL). Wound scratches were captured by inverted light microscope (Carl Zeiss, Oberkochen, Germany) after 24 h and the width of scratch was measured by Image J software (NIH, Bethesda, MD, USA).

In transwell migration assay, suspended cells (at a density of 2×10^5 cells/mL in 100 μL of FBS-free medium) were seeded into upper chamber of 8 μm pores Transwell inserts (Corning, NY, USA), while αMEM with or without EVs (20 μg/mL) were contained in lower chambers. Cells on top chamber were fixed with 4% paraformaldehyde after 24 h and stained with 0.1% crystal violet solution. The cells left on top membrane were gently removed with cotton swabs, and those migrated cells were captured and counted under an inverted light microscope (Carl Zeiss, Oberkochen, Germany).

Odontoblastic differentiation assays

SCAPs were cultured in odontogenic induction medium (OS): α-MEM containing 8% FBS, 1% antibiotics, 10 mM β-glycerophosphate, 0.2 mM ascorbic acid, and 0.1 mM dexamethasone (Sigma-Aldrich, St. Louis, MO, USA). The induction medium was changed every 2 days. Cells were harvested for western blot, qRT-PCR, alizarin red staining, ALP staining and activity assays at certain days.

Alizarin red staining was utilized to identify mineralization nodules formation. SCAPs that were cultured in OS medium for 7 or 14 days, with or without Nor-EV (10 μg/mL), four types LPS-EV (10 μg/mL), NFIC-EV (20 μg/mL), NC-EV (20 μg/mL), were firstly fixed with 4% paraformaldehyde, then, stained with alizarin red staining solution (Cyagen, Guangzhou, China). Mineralization nodules were scanned with phase-contrast microscope (Zeiss, Jena, Germany), subsequently, quantified by absorbance of supernatant at 520 nm after incubating with 0.1 M hexadecylpyridinium chloride monohydrate (Sigma-Aldrich, St. Louis, MO, USA) for 30 min. To detect alkaline phosphatase activity, SCAPs were cultured in OS medium for 3 days, ALP activity of cellular lysates was measured using the ALP activity detection kit (Beyotime, Shanghai, China) according to manufacturer's instructions. ALP activity was normalized to total cell protein concentration by BCA protein assay kit (Cwbio, Beijing, China). As for ALP staining, SCAPs were cultured in OS for 7 days and were fixed with 4% paraformaldehyde for 30 min, then stained with ALP staining solution (Beyotime, Shanghai, China) for 5 min. Mineralized nodules were scanned by phase-contrast microscope (Zeiss, Jena, Germany).

Lentivirus transfection

Lentivirus to overexpress rat and human NFIC and control plasmid DNA were designed and constructed (Hanbio, Shanghai, China). Lentivirus was utilized to transfect SCAPs (MOI = 35) and 293T cell line (MOI = 20) at 50%–60% confluence with the incubation of 4 μg/mL Polybrene (Hanbio, Shanghai, China). Then, cells were cultured in media containing 2 μg/mL puromycin (Hanbio, Shanghai, China) for 24 h. qRT-PCR and Western blot analysis were utilized to analyze the transfection efficacy of NFIC at the mRNA and protein levels, respectively. The NFIC transfected cells were used for subsequent assays.

Western blot analysis

Total protein of cells and EVs was extracted using RIPA lysis buffer (Cwbio, Beijing, China) with protease and phosphatase inhibitors (Cwbio, Beijing, China) and its concentration was measured by BCA protein assay kit (Cwbio, Beijing, China). Proteins were separated on 4%–12% SDS-PAGE gel (SurePAGE™, GenScript, Nanjin, China) and transferred to PVDF membranes (Millipore, Bedford, MA, USA). After blocking with 5% milk for 1 h at room temperature, PVDF membrane were incubated overnight at 4°C with following primary antibodies: anti-NFIC antibody (1:1000, Abcam, Burlingame, CA, USA), anti-DSPP antibody (1:500, sc-73632, Santa Cruz, CA, USA), anti-DMP1 antibody (1:1000, NBP 1-45525, Novus Biologicals, Littleton, CO, Massachusetts, USA), anti-Cyclin D1 (I:1000, #2922, Cell Signaling Technology, Massachusetts, USA), anti-CDK2 (I:1000, #2546, Cell Signaling Technology, Massachusetts, USA), anti-CDK4 (I:1000, #12790, Cell Signaling Technology, Massachusetts, USA), and mouse anti-β-actin (1:1000, AF0003, Beyotime, Shanghai, China). The membranes were incubated with HRP-conjugated secondary antibodies (1:1000, Beyotime, Shanghai, China) at room temperature for 1 h. The immunoreactive bands were incubated with chemiluminescence detection reagents (Millipore, Temecula, MA, USA) and visualized using an ImageQuant LAS 4000mini system (GE Healthcare Life Sciences, Chicago, IL, USA). The intensities of the bands were quantified with software ImageJ (NIH, Bethesda, MD, USA).

Real-time quantitative PCR

Total RNA was extracted from cultured cells using a commercial RNA-Quick purification kit (YISHAN Biotechnology, Shanghai, China) according to its instructions. cDNA was synthesized using PrimeScript™ RT Master Mix Kit (TaKaRa, Dalian, Japan) and then amplified with SYBR Green I Master Mix (Roche, Basel, Switzerland) by the LightCycler 480 Real-Time PCR System (Roche, Basel, Switzerland). The relative mRNA expression of target genes was normalized to β-actin. The specific primers used for detecting mRNA are listed in Table 1.

Table 1. Real-time PCR primers.

Gene	Species	Forward primers, 5′–3′	Reverse primers, 5′–3′
DSPP	Rat	ACAGCGACAGCGACGATTC	CCTCCTACGGCTATCGACTC
DMP-1	Rat	CTGGTATCAGGTCGGAAGAATC	CTCTCATTAGACTCGCTGTCAC
ALP	Rat	GGAAGGAGGCAGGATTGA	TCAGCAGTAACCACAGTCA
NFIC	Rat	ATGTATTCCTCCCCGCTCTGCC	CGGGTTGGACAGCACACAGC
β-actin	Rat	CAGCACTGTGTTGGCATA	CGGTCAGGTCATCACTATC
NFIC	Human	GCGGCGATTACTACACTTC	CTTGTCCATCTCTGTCTTCTTC
β-actin	Human	CATTGCTGACAGGATGCAGA	CTGCTGGAAGGTGGACAGTGA

Histological and immunohistochemistry analysis

The mandibles of apical periodontitis rat model and transplanted scaffold tissues were dissected and fixed in 4% buffered paraformaldehyde for 24 h, then decalcified with 10% ethylenediaminetetraacetic acid (EDTA) for 2 months, dehydrated in a gradient alcohol series, and embedded in paraffin. Subsequently, tissue samples were cut into 4-μm thick sections. Immunohistochemistry (IHC) staining was done using Histostain-SP (Streptavidin-Peroxidase) kit (Bioss, Beijing, China) according to manufacturer's protocols. Sections were deparaffinized, heat retrieved, blocked, and thereafter incubated with the primary antibodies: anti-DMP1 antibody (1:200, NBP 1-45525, Novus Biologicals, Littleton, CO, USA), anti-TNF-a antibody (1:200, bs-10802R, Bioss, Beijing, China), anti-Caspase3 antibody (1:100, GB11009-1, Servicebio, Wuhan, China), anti-CD63 antibody (1:200, DF2305, Affinity Biosciences, OH, USA), overnight at 4°C, followed by washing and incubation with HRP-conjugated secondary antibodies. Signals were visualized with DAB staining. For histological analysis, sections were stained with HE and Masson's trichrome staining solution. For quantitative analysis of Masson's trichrome staining, the blue-stained collagen fiber area was quantified using software ImageJ (NIH, Bethesda, MD, USA) and divided by total tissue area to calculate the collagen volume fraction ($n = 3$). For quantitative analysis of IHC staining, the number of brown-stained cells was divided by total cell number in the observed area to calculate the percentage of CD63/TNF-a/Caspase3/DMP-1 positive cells ($n = 3$).

Cell seeding and in vivo transplantation

To detect the effects of EVs on dentin formation in vivo, SCAPs were loaded onto sterile gelatin scaffolds (5 mm × 3 mm × 2 mm, Dingan Technology Co., Ltd., Suzhou, China) and were assigned to three treatment groups: bare SCAPs-loaded scaffold, NFIC-EV + SCAPs-loaded scaffold, NC-EV + SCAPs-loaded scaffold. Prior to cell seeding, gelatin scaffolds were pre-wetted with medium for 30 min and then immersed in 1 μg/μL EV solution (250 μL/scaffold) for 12 h at 4°C as previously described.[24] Forty microliter of SCAPs suspension (1×10^7 cells/mL) then were added onto EV-loaded scaffolds. After 3 h for cell attachment, 12-well culture plates containing scaffolds (1 disk/well) were filled with 2.5 mL of culture medium/well for 24 h. The gelatin scaffolds with SCAPs were subcutaneously transplanted into nude mice for 8 weeks as described.[25] The rats were anesthetized with Thiopental (0.2 mL/100 g body weight) and sacrificed by exsanguination ($n = 4$, each group).

Statistical analysis

All acquired data are tested by triplicate independent experiments and presented as the mean ± standard deviation. Differences between two groups were examined by Student's *t* test (normal distribution) or Mann-Whitney's *U* test (nonnormal distribution). Multiple group comparisons were conducted by one-way analysis of variance (normal distribution and homogeneity of variance) or Kruskal-Wallis *H*-test (nonnormal distribution or heterogeneity of variance). Statistical analysis was performed using SPSS 22.0 software (SPSS, Inc., Chicago, IL, USA) and $p < 0.05$ was considered statistically significant.

Results

Elevated expression of EV marker CD63 in rat inflamed apical papilla and establishment of in vitro model

Rat model of AP in immature permanent teeth was successfully constructed, which was identified with inflammatory cell infiltration by HE staining (Figure 1(a)) and higher expression of caspase-3 and TNF-α in inflamed apical papilla by IHC staining (Figure 1(b)–(d)). Notably, the significantly increased expression of EV marker CD63 was observed in inflamed apical papilla using IHC staining (Figure 1(b)–(d)), which suggest that EV involves in AP of immature permanent teeth and may regulate AP progression. The progression of AP is the gradual spreading of infections from crown-part pulp tissue to root part of the apical papilla.[26] It was recognized that DPCs are the major cells of pulp tissue, which play important roles in self-defense and repair functions during the progression

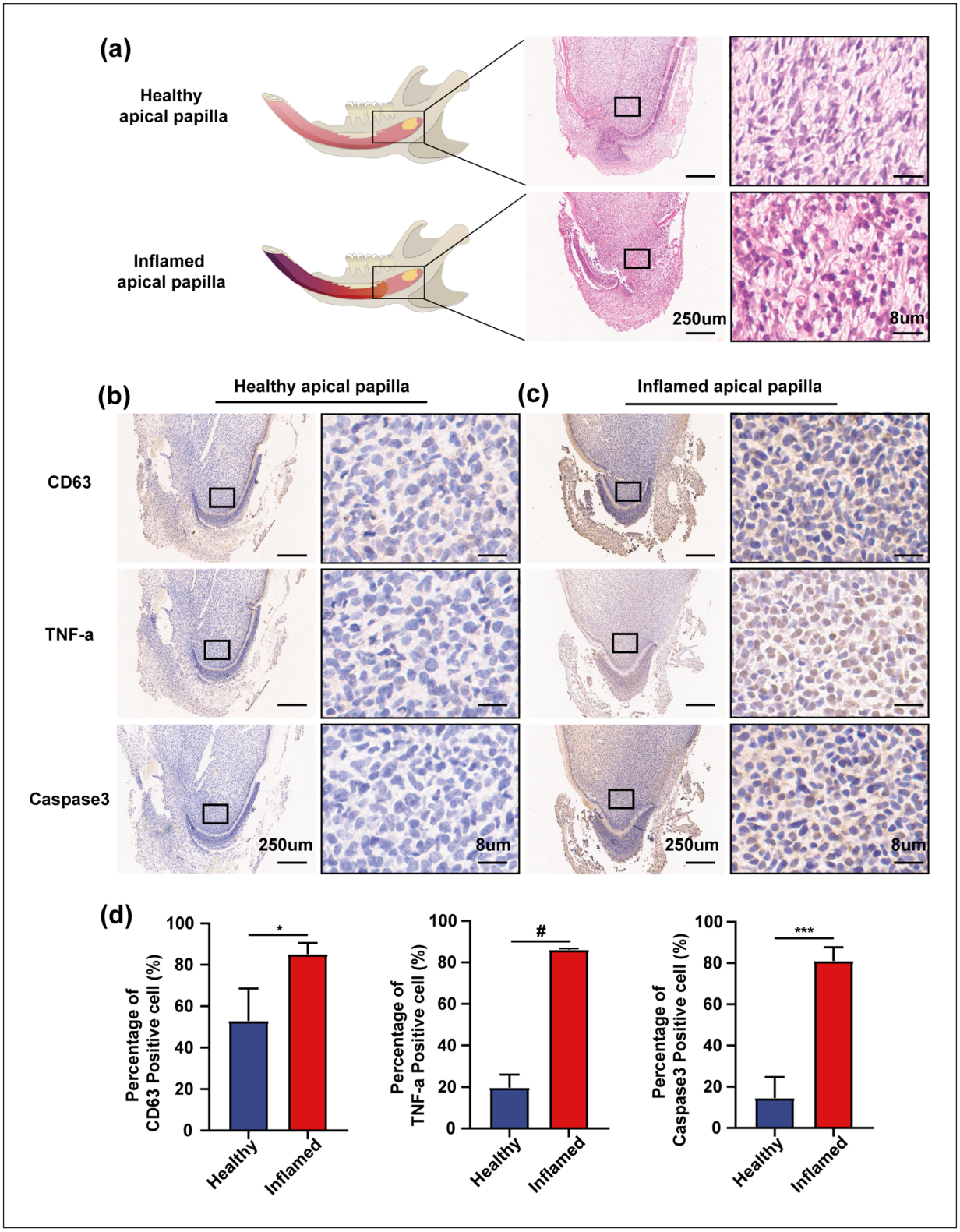

Figure 1. Higher expression of EV surface marker CD63 in apical papilla of rat apical periodontitis model. (a) Schematic diagram showing observed region of apical papilla in apical periodontitis model and healthy control, and HE staining showing inflammatory cell infiltration in inflamed apical papilla ($n = 3$). (b and c) Apical papilla from healthy and inflamed mandibular incisors ($n = 3$) was examined using immunohistochemical staining. Expression of CD63 (EV surface marker), caspase-3, and tumor necrosis factor-a (TNF-a) could barely be detected within healthy apical papilla (left). Significant upregulation of CD63, caspase-3, and TNFa were observed in inflamed apical papilla (right). (d) Quantitative analysis of percentage of CD63/TNFa/Caspase3 positive cell was shown ($n = 3$). *$p < 0.05$. ***$p < 0.001$. #$p < 0.0001$.

of pulpitis,[26] while SCAPs reside in apical papilla of immature permanent teeth, which are critical for tooth root development.[4] To further explore the role of pulp inflammatory EVs in AP and tooth root development, we established the in vitro model using DPCs and SCAPs, and subsequently collected the EVs secreted from LPS-stimulated DPCs and analyzed their effects on cell viability and odontoblastic differentiation of SCAPs. Rat DPCs and SCAPs were successfully cultured and characterized (Supplemental Figure 1).

Identification of EVs derived from LPS-treated DPCs (LPS-EVs)

Effects of LPS on cell viability (Figure 2(a)) and EV secretion (Figure 2(b)) of DPCs were detected, which revealed that 1 μg/mL LPS induced significantly higher EV secretion than that of control group ($p < 0.05$). Four types of EVs derived from DPCs were then collected for following assay: Nor-EV (Culture medium), LPS0.1-EV (Culture medium + 0.1 μg/mL LPS), LPS1-EV (Culture medium + 1 μg/mL LPS), LPS10-EV (Culture medium + 10 μg/mL LPS) (Figure 2(c)). To identify the extracted EVs, Nanoparticle tracing assay (NTA) were performed, which revealed that collected EVs mainly ranged from 30 to 140 nm in diameter with distribution peaks approximately at 100 nm (Figure 2(d)). Scanning electronic microscope (SEM) confirmed the cup-shaped morphology of EVs with a bilayer membrane structure (Figure 2(e)). Moreover, western blot analysis demonstrated the presence of EVs surface marker CD9, CD63, CD81, and TSG101 in collected EVs (Figure 2(g)). To investigate whether collected EVs can be endocytosed by recipient cells, PKH26-labeled EVs were incubated with SCAPs for 48 h. Immunofluorescence staining confirmed that PKH26-labeled EVs were internalized by SCAPs and located in cytoplasm or around nucleus (Figure 2(f)). The effects of four types EVs on cell viability of SCAPs were examined by CCK8 (Figure 2(h)).

LPS-EVs suppressed odontoblastic differentiation and downregulated NFIC in SCAPs

To investigate the effects of four types EV on odontoblastic differentiation of SCAPs, SCAPs were cultured in OS medium with or without 10 μg/mL EVs for 3, 7, and 14 days. After induction for 7 days (Figure 3(a) and (b)) and 14 days (Figure 3(c) and (d)), Alizarin red staining and quantification results revealed that LPS0.1-EV ($p < 0.0001$), LPS1-EV ($p < 0.0001$), and LPS10-EV ($p < 0.0001$) decreased mineralized nodules formation of SCAPs compared with OS group. After induction for 3 days (Figure 3(f)) and 7 days (Figure 3(e)), ALP activity detection and staining identified that LPS0.1-EV ($p < 0.01$), LPS1-EV and LPS10-EV ($p < 0.05$) suppressed alkaline phosphatase activity of SCAPs. Western blot analysis (Figure 3(g) and (h)) showed that LPS10-EV downregulated protein expressions of odontoblastic differentiation markers DSPP ($p < 0.05$) and DMP1 ($p < 0.05$). Considering the critical roles of transcription factor NFIC in tooth root development and odontoblastic differentiation,[27] we also detected the change of NFIC protein level. It was revealed that LPS10-EV downregulated NFIC ($p < 0.05$) of SCAPs after induction for 7 days (Figure 3(g) and (h)), meanwhile, we also found that LPS1-EV ($p < 0.01$) and LPS10-EV ($p < 0.01$) downregulated NFIC protein level of SCAPs when cultured in growth medium for 3 days (Figure 3(i) and (k)). After induction for 7 days, qRT-PCR results (Figure 3(j)) showed that LPS0.1-EV, LPS1-EV, and LPS10-EV inhibited expression of odontogenic marker DMP1, ALP, and transcription factor NFIC in SCAPs.

NFIC overexpression ameliorated LPS-EVs-induced suppression on odontoblastic differentiation

It was reported that NFIC regulates the expression of DSPP and DMP-1 during odontoblast differentiation.[27] To investigate whether LPS-EVs suppress odontoblastic differentiation via downregulating NFIC, NFIC was overexpressed in SCAPs by lentivirus transfection. Overexpression efficiency of NFIC was confirmed by qRT–PCR ($p < 0.001$) and western blot analysis ($p < 0.01$) (Figure 4(a)). Both of SCAPs that overexpressing NFIC (OE-NFIC-SCAPs) or transfected with blank control plasmid DNA (NC-NFIC-SCAPs) were cultured in OS medium with or without 10 μg/mL EVs for certain time interval (3 or 7 days) (Figure 4(b)–(k)). After induction for 7 days, Alizarin red staining and quantification revealed that LPS0.1-EV ($p < 0.05$), LPS1-EV ($p < 0.0001$), and LPS10-EV ($p < 0.0001$) decreased mineralized nodules formation in NC-NFIC-SCAPs group (Figure 4(b) and (c)), while there was no difference between LPS0.1-EV, LPS1-EV, LPS10-EV group and OS group in OE-NFIC-SCAPs (Figure 4(d) and (e)). Similarly, compared with OS group, LPS0.1-EV ($p < 0.01$), LPS1-EV ($p < 0.0001$), and LPS10-EV ($p < 0.0001$) suppressed ALP activity of NC-NFIC-SCAPs after induction for 3 days (Figure 4(f)), while there was no significant difference between LPS0.1-EV, LPS1-EV group and OS group in OE-NFIC-SCAPs (Figure 4(g)). Western blot analysis also identified that LPS10-EV suppressed protein expression of DSPP ($p < 0.0001$) and DMP-1 ($p < 0.05$) in NC-NFIC-SCAPs after induction for 7 days (Figure 4(h) and (j)), while there was no difference between LPS-EVs group and OS group in OE-NFIC-SCAPs (Figure 4(i) and (k)).

Construction of NFIC-EV for encapsulating and delivering NFIC

To exploit EV for delivery of NFIC, as shown in schematic diagram (Figure 5(a)), NFIC-encapsulated EV

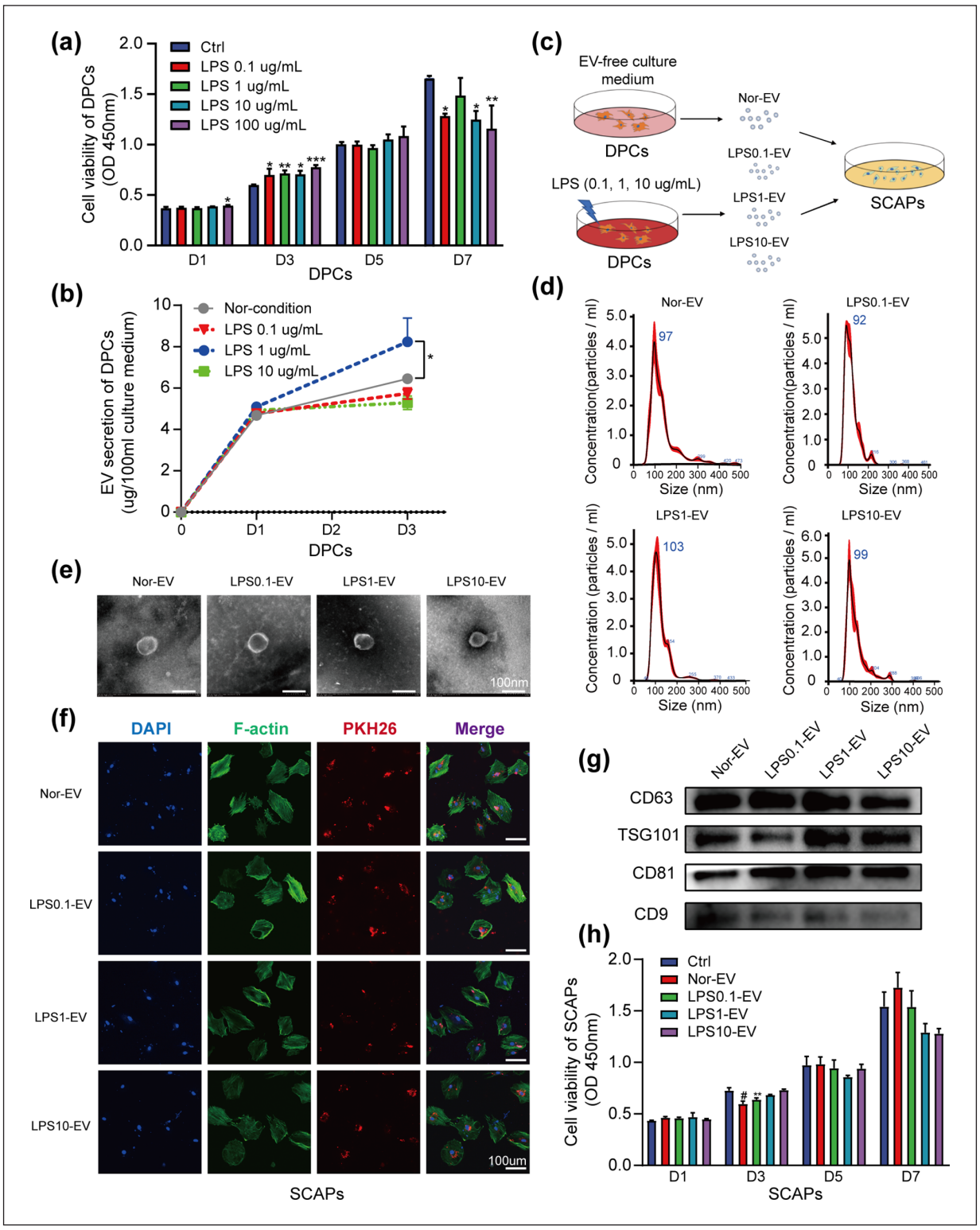

Figure 2. Identification of EVs derived from LPS-stimulated DPCs (LPS-EVs) and establishment of in vitro model. (a) CCK8 assay detected cell viability of DPCs treated LPS (0.1, 1, 10, 100 μg/mL). (b) 1 μg/mL LPS increased EVs secretion of DPCs, compared to the other groups. (c) Schematic diagram shows the four types EV collected from EV-free culture medium of DPCs with or without LPS stimulation (0.1, 1, 10 μg/mL), which were used in subsequent assays. (d) Nanoparticle tracing assay (NTA) revealed the diameter of collected EVs was approximately 100 nm. (e) Scanning electron microscopy (SEM) of cup and saucer-shaped EVs. (f) Immunofluorescence staining confirmed that PKH26-labeled EVs (red) were endocytosed by SCAPs. DAPI (blue), and F-actin (green). (g) Western blot analysis of EVs surface markers (CD9, CD63, CD81 and TSG101). (h) CCK8 assay detected the effect of Nor-EV and LPS-EVs on cell viability of SCAPs. *$p < 0.05$. **$p < 0.01$. ***$p < 0.001$.#$p < 0.0001$.

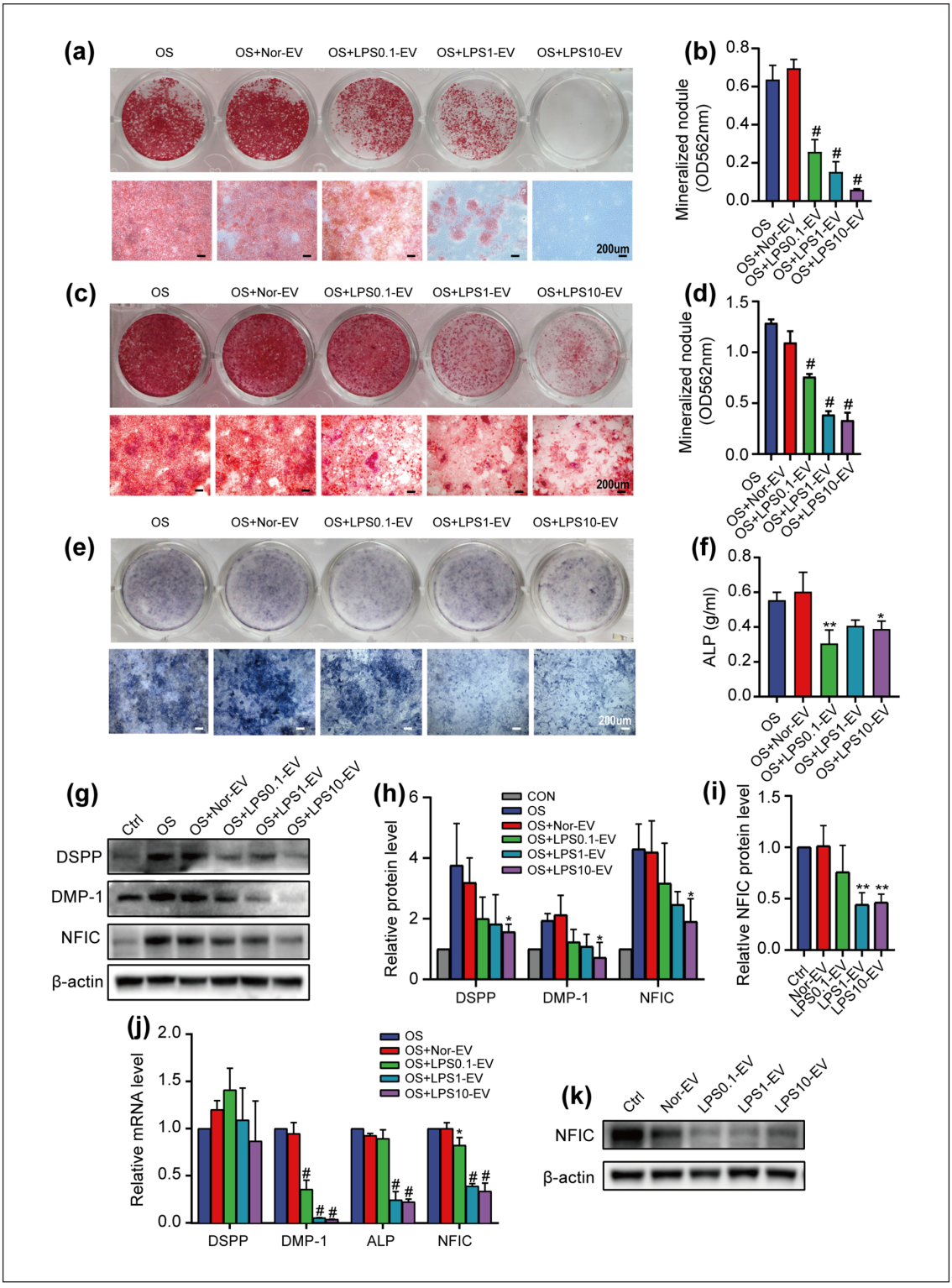

Figure 3. LPS-EVs impairs odontoblastic differentiation and downregulates NFIC in SCAPs. Alizarin Red S staining and quantification assay showed that LPS-EVs suppressed mineralized nodule formation of SCAPs after odontogenic induction for 7 days (a and b) and 14 days (c and d). ALP staining (at day 7) and activity (at day 3) assay showing that LPS-EV suppressed the alkaline phosphatase activity of SCAPs (e and f). (g and h) Western blot analysis identified that LPS-EVs downregulated DSPP, DMP1, and NFIC of SCAPs at a protein level after odontogenic induction for 7 days. (j) RT-qPCR found that LPS-EVs downregulated mRNA expression of odontoblastic markers (DSPP, DMP1, ALP) and NFIC in SCAPs after odontogenic induction for 7 days. (i and k) Treatment of LPS-EVs for 3 days downregulated NFIC expression of SCAPs without osteogenic induction. *$p < 0.05$. **$p < 0.01$. #$p < 0.0001$.

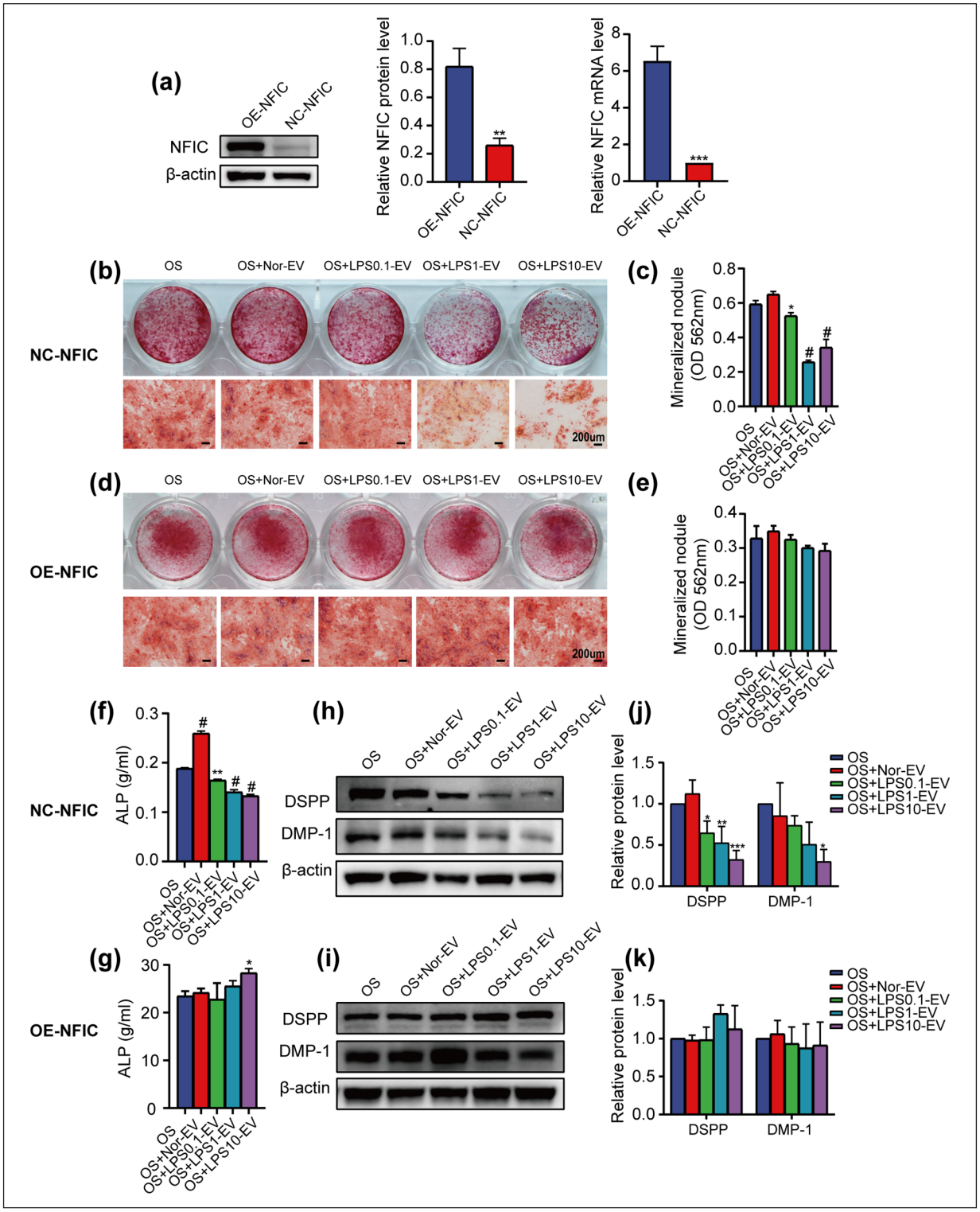

Figure 4. Overexpression of NFIC in SCAPs rescues suppressed odontoblastic differentiation induced by LPS-EVs. (a) qRT-PCR and Western blot analysis identified transfection efficiency of NFIC overexpression. (b and c) Alizarin Red S staining and quantification assay revealed that LPS-EVs suppressed mineralized nodule formation of NC-NFIC SCAPs after odontogenic induction for 7 days, while it was rescued in OE-NFIC SCAPs (d and e). (f and g) ALP activity assay showing NFIC overexpression rescued ALP activity of SCAPs after odontogenic induction for 3 days. (h–k) Western blot analysis identified that NFIC overexpression rescued LPS-EVs-induced downregulation of DSPP, DMP1 protein in SCAPs (induction for 7 days). *$p < 0.05$. **$p < 0.01$. ***$p < 0.001$. #$p < 0.0001$.

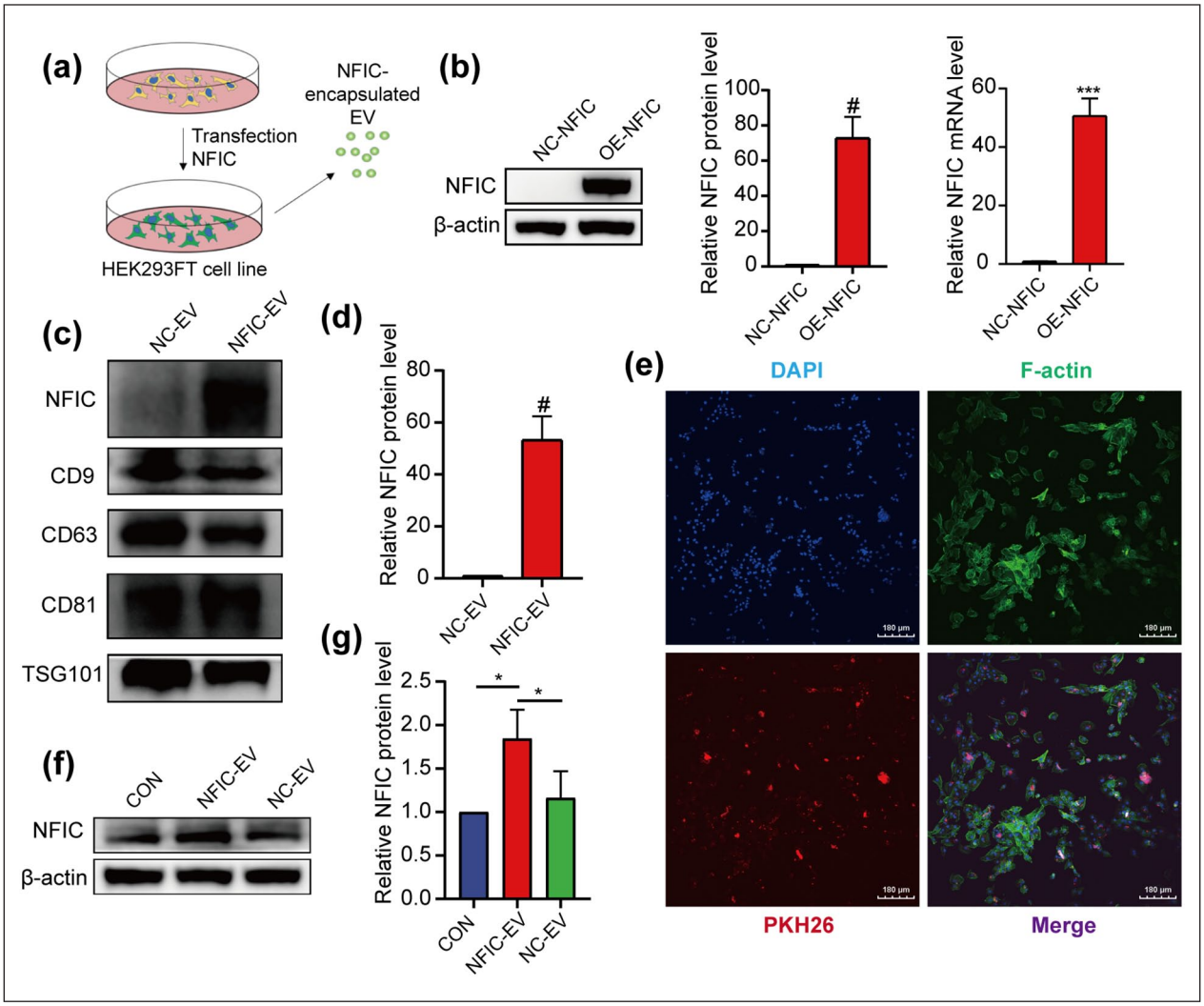

Figure 5. Construction of NFIC-EV for encapsulating and delivering NFIC. (a) Schematic diagram illustrates the method of overexpressing NFIC in HEK293FT cell line to construct NFIC-encapsulated EV. (b) qRT-PCR and Western blot analysis identified transfection efficiency of NFIC in HEK293FT cell. (c and d) Overexpressing NFIC in HEK293FT cells facilitated higher NFIC protein level in EVs derived from HEK293FT cell, which were termed as "NFIC-EV" and used in subsequent assays. Herein, NFIC protein level were normalized to EVs specific markers CD63 (e) PKH26-labeled NFIC-EV were endocytosed by SCAPs. (f and g) Treatment of NFIC-EV for 3 days upregulated NFIC of SCAPs at a protein level. *$p < 0.05$. ***$p < 0.01$. #$p < 0.0001$.

(NFIC-EV) and NC-EV were collected from culture medium of OE-NFIC-HEK293FT and NC-NFIC-HEK293FT cell lines which were constructed by lentivirus transfection.[28] Overexpression efficiency of NFIC was confirmed by qRT–PCR ($p < 0.001$) and Western blot ($p < 0.0001$) (Figure 5(b)). Western blot analysis of EVs lysates revealed that overexpression of NFIC resulted in significantly higher NFIC protein level in EVs ($p < 0.0001$) (Figure 5(c) and (d)), here, the NFIC protein level was normalized to protein level of EVs surface marker CD63 (Figure 5(d)). Immunofluorescence of PKH26-labeled NFIC-EV identified that NFIC-EV were endocytosed by SCAPs (Figure 5(e)), moreover, after incubation for 3 days, NFIC-EV upregulated NFIC protein level ($p < 0.05$) in SCAPs which was examined by Western blot analysis (Figure 5(f) and (g)).

NFIC-EV promoted proliferation and migration of SCAPs

To examine the effects of NFIC-EV on cell proliferation, SCAPs were treated with NFIC-EV (20 μg/mL), NC-EV (20 μg/mL), and PBS for 1, 3, 5, and 7 days (in the absence of LPS). SCAPs that were treated with NFIC-EV exhibited faster proliferation rate than NC-EV and blank control group (Figure 6(a)). After treatment of EVs for 3 days, cell cycle distribution of SCAPs was detected by flow cytometry and NFIC-EV induced a higher S phase proportion in SCAPs ($p < 0.05$) (Figure 6(d) and (e)).

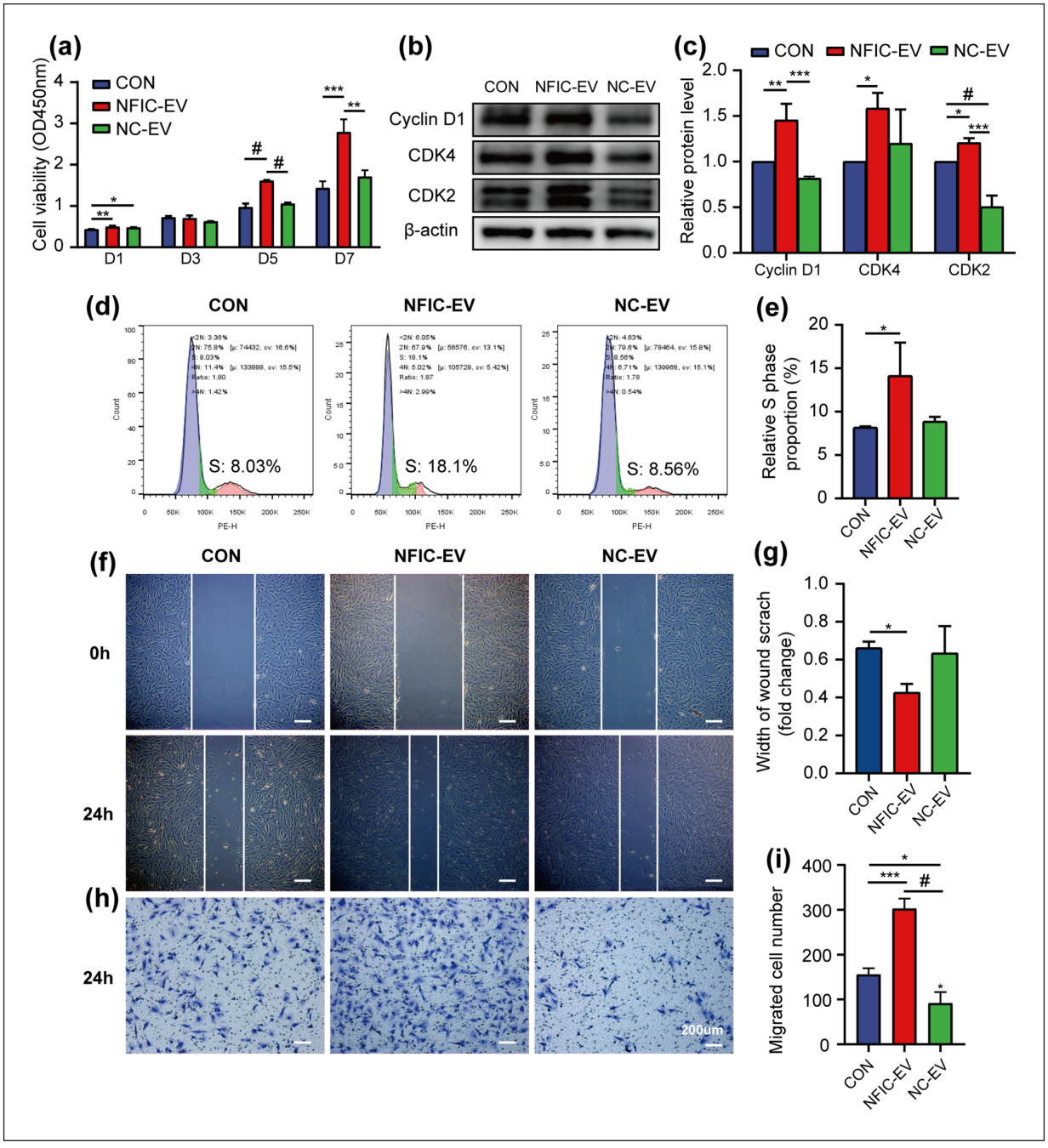

Figure 6. NFIC-EV promotes proliferation and migration of SCAPs. (a) CCK8 assay determined proliferation of SCAPs that were treated with NFIC-EV for 1, 3, 5, 7 days. (b and c) Western blot analysis revealed that incubation of NFIC-EV for 3 days upregulated cell cycle regulator protein (Cyclin D1, CDK4, CDK2) in SCAPs. (d) After treatment with NFIC-EV for 3 days, cell cycle distribution of SCAPs was determined by flow cytometry. (e) Statistical analysis of cell cycle indicates that NFIC-EV induced a higher S phage proportion in SCAPs. (f–i) Migration of SCAPs after treatment with NFIC-EV for 24 h. NFIC-EV promoted migration of SCAPs in wound-healing assay (f and g) and Transwell migration assay (h and i). Assays in this figure are carried out in the absence of LPS, $*p < 0.05$, $**p < 0.01$, $***p < 0.001$, $\#p < 0.0001$.

Moreover, western blot analysis clarified that incubation of NFIC-EVs for 3 days upregulated cell cycle regulator protein (Cyclin D1, CDK4, CDK2, $p < 0.05$) in SCAPs (Figure 6(b) and (c)).

To assess cell migration, NFIC-EV (20 μg/mL), NC-EV (20 μg/mL), and PBS were added to SCAPs (in the absence of LPS). After incubation for 24 h, NFIC-EV promoted migration in both wound-healing assay ($p < 0.05$) (Figure 6(f) and

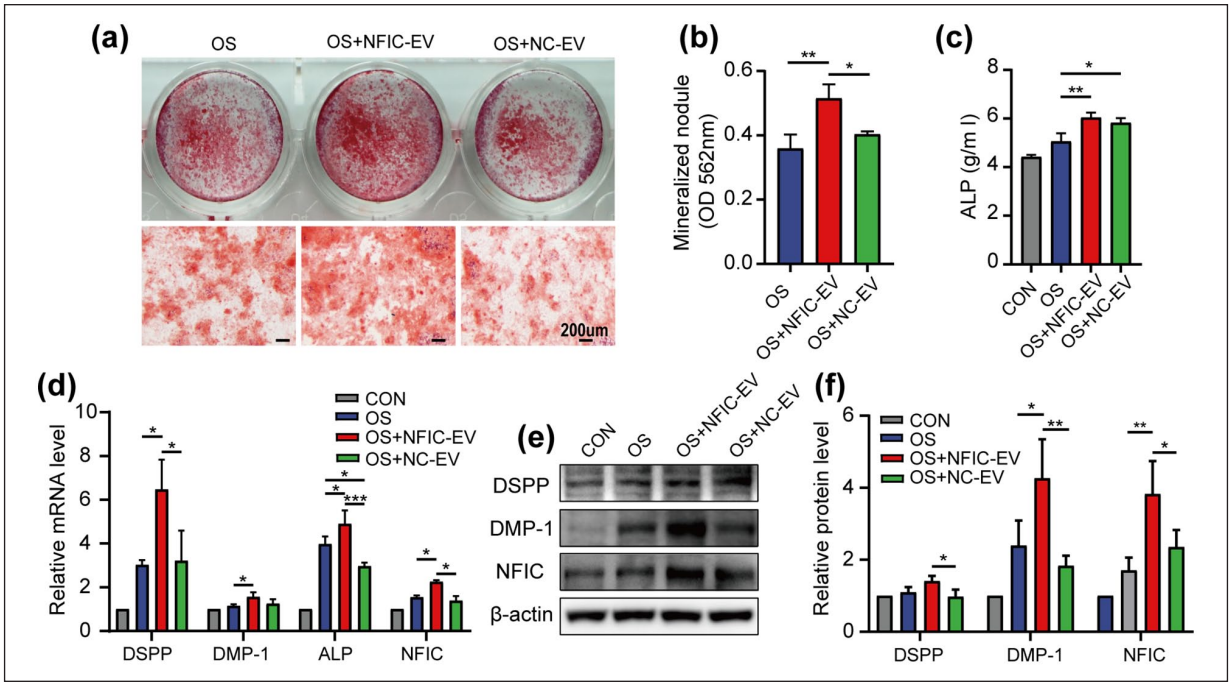

Figure 7. NFIC-EV promotes odontoblastic differentiation of SCAPs in vitro. (a and b) Alizarin Red S staining and quantification assay revealed that NFIC-EV promoted mineralized nodule formation of SCAPs after odontogenic induction for 7 days. (c) Effect of NFIC-EV on ALP activity of SCAPs after odontogenic induction for 3 days. (d) NFIC-EV upregulated odontoblastic markers (DSPP, DMP-1, ALP) and NFIC of SCAPs at mRNA level. (e and f) NFIC-EV upregulated DSPP, DMP-1, and NFIC of SCAPs at a protein level. Assays in this figure are carried out in the absence of LPS, $*p < 0.05$, $**p < 0.01$, $***p < 0.001$.

(g)) and Transwell migration assay ($p < 0.001$) (Figure 6(h) and (i)).

NFIC-EV promoted odontoblastic differentiation of SCAPs in vitro and detinogenesis in vivo

To investigate the effects of NFIC-EV on odontoblastic differentiation of SCAPs, NFIC-EV (20 µg/mL), NC-EV (20 µg/mL), and PBS were added to OS medium (in the absence of LPS). After incubation for 3 days, ALP activity of SCAPs was higher compared to OS group ($p < 0.01$) (Figure 7(c)). After incubation for 7 days, Alizarin Red S staining and quantification indicated that NFIC-EV promoted mineralized nodule formation ($p < 0.01$) (Figure 7(a) and (b)), meanwhile, NFIC-EV upregulated odontoblastic markers (DSPP, DMP-1, ALP) and NFIC ($p < 0.001$) at mRNA level (Figure 7(d)), and DSPP, DMP-1 ($p < 0.05$), and NFIC ($p < 0.01$) at protein level (Figure 7(e) and (f)).

The effects of NFIC-EV on dentin formation in vivo were subsequently assessed. Gelatin scaffolds loaded with: SCAPs, SCAPs + NFIC-EV (250 µL/scaffold), SCAPs + NC-EV (250 µL/scaffold) were transplanted subcutaneously into nude mice for 8 weeks (Figure 8(a)). HE staining (Figure 8(b)), Masson trichrome staining (Figure 8(e)), and quantification of collagen volume fraction (Figure 8(c)) proved that more dentin and collagen were formed in scaffolds loaded with NFIC-EV compared with NC-EV ($p < 0.01$) and control group ($p < 0.0001$). IHC staining (Figure 8(f)) and its quantitative analysis for percentage of DMP-1 positive cells (Figure 8(d)) also demonstrated higher DMP-1 expression occurred in scaffolds loaded with NFIC-EV group compared with NC-EV ($p < 0.01$) and control group ($p < 0.0001$).

Discussion

Defining roles of EV in AP progression, especially in immature teeth, would contribute to prevention and treatment of AP. To the best of our knowledge, this is the first study which assessed the involvement of EV in AP progression and odontoblastic differentiation of SCAPs. In this study, the expression of EV surface marker CD63 was upregulated in inflamed apical papilla of AP model, which indicates that periapical infection increases EV secretion within apical papilla tissue. Given that AP is a chronic inflammatory lesion that usually spread from inflamed pulp tissue, we established the in vitro model and confirmed that LPS-EV derived from DPCs suppressed odontoblastic differentiation of SCAPs through downregulating NFIC, which suggests an inhibitory role of pulp inflammatory EVs in odontoblastic differentiation. Furthermore, for therapeutic purpose, our study here for the first time developed a NFIC-encapsulated EV to deliver and replenish NFIC in

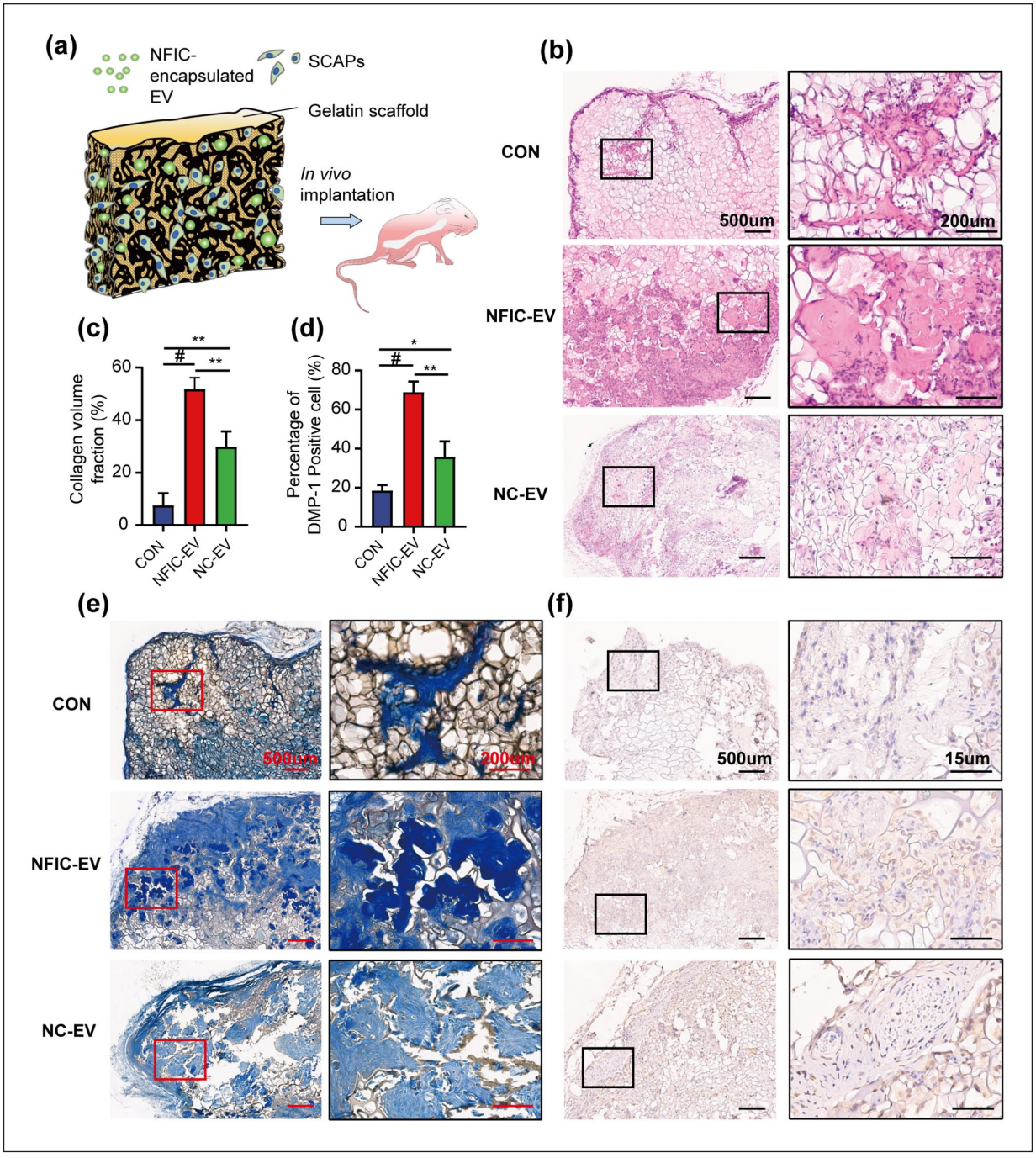

Figure 8. NFIC-EV promotes dentinogenesis of SCAPs in vivo. (a) Schematic model shows gelatin scaffold seeded with SCAPs and loaded with NFIC-EV, NC-EV ($n = 4$), which were subcutaneously transplanted in nude mice for 8 weeks. Representative image of HE staining (b) and Masson trichrome staining (e) show that NFIC-EV promoted dentin and collagen formation in vivo. (f) Representative image of IHC staining of DMP-1 in regenerated tissues. Quantitative analysis of collagen volume fraction (c) and percentage of DMP-1 positive cells (d) was shown. *$p < 0.05$. **$p < 0.01$. #$p < 0.0001$.

SCAPs, hopefully, exploiting EV as a potential strategy for treatment of AP and dentin regeneration.

As critical effectors of paracrine function, EVs are being increasingly linked to pathological mechanism of inflammatory diseases. It was discovered that renal EV initiated tubulointerstitial inflammation in acute kidney injury, and EV of LPS-stimulated macrophage promoted the progression of liver fibrosis,[29,30] meanwhile, Ni et al.[31] reported that EVs from osteoarthritic chondrocyte aggravated synovitis in osteoarthritis. EV was also introduced as a novel inflammatory mediator, which could be released into bronchoalveolar lavage fluid and cerebrospinal fluid, causing

pneumonia and neuroinflammation of central nervous system.[32–34] Recently, EVs have gained more attention as a protection or repair mechanism against pulp infection, and it was found that EV derived from LPS-stimulating dental cells protect cells from apoptosis and promote the proliferation, migration, and differentiation of several dental stem cells,[12–15] however, our data here found that EV derived from LPS-stimulated DPCs suppressed odontoblastic differentiation of SCAPs, which suggests a pathological role of EV in AP progression. The paradoxical roles of LPS-stimulated EV can be attributed to the heterogeneity among different subtypes of dental cells-derived EVs,[35] meanwhile, given the variation of LPS concentration and precondition time duration between each study, another explanation is that a different role of LPS-stimulated EVs may be associated with the severity of infection.

Accumulating evidence have confirmed the multiple functions of EVs, which have established their potentials as therapeutic mediators for tissue repair and regeneration,[36] including wound healing,[37] bone and cartilage regeneration,[38,39] bladder transplantation,[40] kidney, and cardiovascular therapeutics.[41,42] As for the application of EVs for dentin regeneration, several studies revealed that exosomes derived from human dental pulp stem cells (DPSCs) and SCAPs could promote dentin-pulp complex regeneration and odontogenic differentiation of DPSCs through TGFβ1/smads and P38/MAPK signaling via transferring microRNAs.[43–45] Zhang and Wang et al.[46,47] also reported that EVs derived from Hertwig's epithelial root sheath cells and Schwann cell were able to promote dentin-pulp complex regeneration. Others explored that DPCs-EV combined with treated dentin matrix (TDM) proteins or the control released vehicle as a bioactive pulp-capping material for reparative dentin formation.[48,49] Compared with previous studies that utilized native EVs from cultured cells, our research here harnesses the bioengineered EVs derived from NFIC-overexpressing cells for the first time, which provides novel ideas for EV-based dentin regeneration.

NFIC is a critical transcription factor for tooth development and bone formation. Deficiency of NFIC contributes to short root anomaly (SRA) and dentin malformation. NFIC interacts with various signal molecules that are essential for osteo-/odontoblastic differentiation, including transforming growth factor-β1, Osterix, Runx2, Krüppel-like factor 4, and β-catenin.[50–52] Moreover, it was verified that NFIC promotes odontoblastic differentiation of SCAPs by upregulating odontoblast-specific protein DSPP, DMP-1, COL-1, OCN, and Nestin, while deficiency of NFIC suppresses the proliferation of odontoblast and induces cell apoptosis,[27,53–55] besides, the anti-inflammatory role of NFIC was also reported in human SCAPs.[56] In our study, we elucidate that LPS-EV robustly downregulated NFIC in SCAPs, which subsequently suppressed odontoblastic differentiation by inhibiting DSPP and DMP-1, moreover, further overexpression of NFIC ameliorated LPS-EV-induced suppression on odontoblastic differentiation. Our findings here not only provide clues regarding the mechanism how LPS-EV suppresses odontoblastic differentiation, but also indicates an EV-dependent possible mechanism by which pulp infection interferes with tooth root development.

Despite extensive researches exploiting EVs as delivery vehicles for tissue engineering, most of them tested their ability to transfer small non-coding RNAs and only a few studies transferring transcription factors are reported.[17] It was reported that Hypoxia-inducible factor-1(HIF-1α)-encapsulated EV derived from mesenchymal stem cells enhanced angiogenesis in myocardial infarction model,[57] and Nuclear factor erythroid 2-related factor 2 (Nrf2)-encapsulated EV was applied to accelerate cutaneous wound healing,[58] meanwhile, Nuclear factor of activated T cells 3 (NFAT3)-encapsulated EV suppressed tumor growth and metastatic dissemination.[59] In this study, based on our evidence that inhibition of odontoblastic differentiation is associated with the decline of NFIC, we proposed that replenishing and delivering NFIC via EV as a promising therapeutic manipulation. Therefore, we developed the NFIC-EV by encapsulating NFIC protein into EV, which were endocytosed and successfully upregulated NFIC level in SCAPs, most importantly, NFIC-EV promoted proliferation, migration, and odontoblastic differentiation of SCAPs in vitro, as well as dentin formation in vivo. Considering the well-defined role of NFIC in tooth and bone development, delivering NFIC via EV might be promising for not only therapy of AP, tooth formation disorders, and skeletal developmental diseases, but also dentin and bone regeneration.

Encapsulating desired cargo via extracellular vesicles can be achieved either endogenously (during EV biogenesis) or exogenously (after EV isolation). Endogenous loading requires modulating donor cells to favor inclusion of selected cargo into extracellular vesicles.[19,60] In the present study, we overexpressed NFIC in HEK293FT cells by direct transfection, subsequently, intracellular NFIC protein was loaded into vesicles through endogenous cellular sorting machinery and secreted into extracellular space. We found that EVs shed by NFIC-overexpressing HEK293FT cells contained a robustly higher level of NFIC protein than blank control EV, suggesting that genetical engineering of donor cells is an effective method for loading transcription factor. Another important consideration for endogenous loading is donor cell type, we here chose the HEK293FT cell as producer cell for its high transfection efficacy, high EV productivity, as well as its readily-accessibility.[28] In the future, further improvements to increase encapsulation efficiency and EV production are still needed in order to successfully exploiting EV delivery for tissue engineering.

Conclusion

Our findings elucidate not only the presence and increased production of extracellular vesicle during apical periodontitis progression but also its regulatory roles in odontoblastic differentiation. The inhibition of odontoblastic differentiation in SCAPs induced by pulp inflammatory EV is mediated through downregulating NFIC, which indicates a possible EV-dependent mechanism in pathophysiology of apical periodontitis. More importantly, our attempt to exploit EV for delivering NFIC, a critical transcription factor for tooth development and bone formation, promotes proliferation, migration of SCAPs and dentinogenesis both in vitro and in vivo, which provides a novel potential strategy for clinical therapeutics and dentin regeneration.

Acknowledgements

The authors would like to thank the Guangdong Provincial Key Laboratory of Stomatology, Sun Yat-sen University, for providing all experimental equipments. The authors would like to thank Jun Kang, Haolin Chen, Tong Yan, Jingzhou Li, Lv Xie, Shuxiang Lei, Jinyan Wu, Mengjie Li, Cheng Xu, Weiyang Chen, Mingmei Yang, Zelin Liang, Baoyu Li, Yongjie Cai, Yiping Kong (Guangdong Provincial Key Laboratory of Stomatology) for technical help and general support during experiments conduction, and Suyu Wang (University of Hongkong) for critical reading.

Author contributions

Shengyan Yang contributed to conception, design, data acquisition, analysis, interpretation, draft, and revision of manuscript; Qing Liu and Fuping Zhang contributed to study design, data acquisition, and revision of manuscript; Shijing Chen data analysis and interpretation, revision of manuscript; Yaoyin Li and Wenguo Fan contributed to study design, supervision, and revision of manuscript; Lijia Mai contributed to data acquisition; Fang Huang and Hongwen He contributed to funding acquisition, study design, supervision, revision, and submission of manuscript. All authors gave final approval and agreed to be accountable for all aspects of the work.

Declaration of conflicting interests

The author(s) declared no potential conflicts of interest with respect to the research, authorship, and/or publication of this article.

Funding

The author(s) disclosed receipt of the following financial support for the research, authorship, and/or publication of this article: The author(s) disclosed receipt of the following financial support for the research, authorship, and/or publication of this article: This work was supported by grants from the National Natural Science Foundation of China (No. 81870737, No.81771098, and No. 81972545), Natural Science Foundation of Guangdong Province (No. 2021A1515011779), Science and Technology Planning Project of Guangzhou City (No. 202102020147), and was partly supported by the Guangdong Financial Fund for High-Caliber Hospital Construction (174-2018-XMZC-0001-03-0125/D-02).

ORCID iD

Shengyan Yang https://orcid.org/0000-0003-1211-7495

Supplemental material

Supplemental material for this article is available online.

References

1. Tibúrcio-Machado CS, Michelon C, Zanatta FB, et al. The global prevalence of apical periodontitis: a systematic review and meta-analysis. *Int Endod J* 2021; 54: 712–735.
2. Hargreaves KM, Diogenes A and Teixeira FB. Treatment Options: biological basis of regenerative endodontic procedures. *J Endod* 2013; 39: S30–S43.
3. Huang GT, Sonoyama W, Liu Y, et al. The hidden treasure in apical papilla: the potential role in pulp/dentin regeneration and bioroot engineering. *J Endod* 2008; 34: 645–651.
4. Kang J, Fan W, Deng Q, et al. Stem cells from the apical papilla: A promising source for stem cell-based therapy. *Biomed Res Int* 2019; 2019: 6104738.
5. van Niel G, D'Angelo G and Raposo G. Shedding light on the cell biology of extracellular vesicles. *Nat Rev Mol Cell Biol* 2018; 19: 213–228.
6. Kalluri R and LeBleu VS. The biology, function, and biomedical applications of exosomes. *Science* 2020; 367: 640.
7. Zhang H, Wang L, Li C, et al. Exosome-induced regulation in inflammatory bowel disease. *Front Immunol* 2019; 10: 1464.
8. Tavasolian F, Moghaddam AS, Rohani F, et al. Exosomes: Effectual players in rheumatoid arthritis. *Autoimmun Rev* 2020; 19: 102511.
9. Pérez PS, Romaniuk MA, Duette GA, et al. Extracellular vesicles and chronic inflammation during HIV infection. *J Extracell Vesicles* 2019; 8: 1687275.
10. Lee H, Abston E, Zhang D, et al. Extracellular vesicle: an emerging mediator of intercellular crosstalk in lung inflammation and injury. *Front Immunol* 2018; 9: 924.
11. Xing X, Han S, Li Z, et al. Emerging role of exosomes in craniofacial and dental applications. *Theranostics* 2020; 10: 8648–8664.
12. Wang HS, Yang FH, Wang YJ, et al. Odontoblastic exosomes attenuate apoptosis in neighboring cells. *J Dent Res* 2019; 98: 1271–1278.
13. Shi W, Guo S, Liu L, et al. Small extracellular vesicles from lipopolysaccharide-preconditioned dental follicle cells promote periodontal regeneration in an inflammatory microenvironment. *ACS Biomater Sci Eng* 2020; 6: 5797–5810.
14. Li J, Ju Y, Liu S, et al. Exosomes derived from lipopolysaccharide-preconditioned human dental pulp stem cells regulate Schwann cell migration and differentiation. *Connect Tissue Res* 2021; 62: 277–286.
15. Chen W-J, Xie J, Lin X, et al. The role of small extracellular vesicles derived from lipopolysaccharide-preconditioned human dental pulp stem cells in dental pulp regeneration. *J Endod* 2021; 47: 961–969.
16. Tsiapalis D and O'Driscoll L. Mesenchymal stem cell derived extracellular vesicles for tissue engineering and regenerative medicine applications. *Cells* 2020; 9: 991.

17. O'Brien K, Breyne K, Ughetto S, et al. RNA delivery by extracellular vesicles in mammalian cells and its applications. *Nat Rev Mol Cell Biol* 2020; 21: 585–606.
18. Tran PHL, Xiang D, Tran TTD, et al. Exosomes and nanoengineering: A match made for precision therapeutics. *Adv Mater* 2020; 32: e1904040.
19. Herrmann IK, Wood MJA and Fuhrmann G. Extracellular vesicles as a next-generation drug delivery platform. *Nat Nanotechnol* 2021; 16: 748–759.
20. Renard E, Gaudin A, Bienvenu G, et al. Immune cells and molecular networks in experimentally induced pulpitis. *J Dent Res* 2016; 95: 196–205.
21. Gao Q, Ge J, Ju Y, et al. Roles of L-type calcium channels (Ca(V)1.2) and the distal C-terminus (DCT) in differentiation and mineralization of rat dental apical papilla stem cells (rSCAPs). *Arch Oral Biol* 2017; 74: 75–81.
22. Hong H, Chen X, Li K, et al. Dental follicle stem cells rescue the regenerative capacity of inflamed rat dental pulp through a paracrine pathway. *Stem Cell Res Ther* 2020; 11: 333.
23. Lin Y, Nan J, Shen J, et al. Canagliflozin impairs blood reperfusion of ischaemic lower limb partially by inhibiting the retention and paracrine function of bone marrow derived mesenchymal stem cells. *EBioMedicine* 2020; 52: 102637.
24. Li W, Liu Y, Zhang P, et al. Tissue-engineered bone immobilized with human adipose stem cells-derived exosomes promotes bone regeneration. *ACS Appl Mater Interfaces* 2018; 10: 5240–5254.
25. Zhou C, Yang G, Chen M, et al. Lhx8 mediated Wnt and TGFβ pathways in tooth development and regeneration. *Biomaterials* 2015; 63: 35–46.
26. Yu C and Abbott PV. An overview of the dental pulp: its functions and responses to injury. *Aust Dent J* 2007; 52: S4–S16.
27. Xu C, Xie X, Zhao L, et al. The critical role of nuclear factor I-C in tooth development. *Oral Dis* 2021 Oct 12. doi: 10.1111/odi.14046. Epub ahead of print. PMID: 34637578.
28. Lin Y, Wu J, Gu W, et al. Exosome-liposome hybrid nanoparticles deliver CRISPR/Cas9 system in MSCs. *Adv Sci* 2018; 5: 1700611.
29. Chen L, Yao X, Yao H, et al. Exosomal miR-103-3p from LPS-activated THP-1 macrophage contributes to the activation of hepatic stellate cells. *FASEB J* 2020; 34: 5178–5192.
30. Lv LL, Feng Y, Wu M, et al. Exosomal miRNA-19b-3p of tubular epithelial cells promotes M1 macrophage activation in kidney injury. *Cell Death Differ* 2020; 27: 210–226.
31. Ni Z, Kuang L, Chen H, et al. The exosome-like vesicles from osteoarthritic chondrocyte enhanced mature IL-1β production of macrophages and aggravated synovitis in osteoarthritis. *Cell Death Discov* 2019; 10: 522.
32. Balusu S, Van Wonterghem E, De Rycke R, et al. Identification of a novel mechanism of blood-brain communication during peripheral inflammation via choroid plexus-derived extracellular vesicles. *EMBO Mol Med* 2016; 8: 1162–1183.
33. Li JJ, Wang B, Kodali MC, et al. In vivo evidence for the contribution of peripheral circulating inflammatory exosomes to neuroinflammation. *J Neuroinflammation* 2018; 15: 8.
34. Lee H, Zhang D, Laskin DL, et al. Functional evidence of pulmonary extracellular vesicles in infectious and noninfectious lung inflammation. *J Immunol* 2018; 201: 1500–1509.
35. Li Y, Duan X, Chen Y, et al. Dental stem cell-derived extracellular vesicles as promising therapeutic agents in the treatment of diseases. *Int J Oral Sci* 2022; 14: 2.
36. Nagelkerke A, Ojansivu M, van der Koog L, et al. Extracellular vesicles for tissue repair and regeneration: evidence, challenges and opportunities. *Adv Drug Deliv Rev* 2021; 175: 113775.
37. Kim H, Wang SY, Kwak G, et al. Exosome-guided phenotypic switch of M1 to M2 macrophages for cutaneous wound healing. *Adv Sci* 2019; 6: 1900513.
38. Jin Q, Li P, Yuan K, et al. Extracellular vesicles derived from human dental pulp stem cells promote osteogenesis of adipose-derived stem cells via the MAPK pathway. *J Tissue Eng* 2020; 11: 2041731420975569.
39. Cui S and Zhang L. microRNA-129-5p shuttled by mesenchymal stem cell-derived extracellular vesicles alleviates intervertebral disc degeneration via blockade of LRG1-mediated p38 MAPK activation. *J Tissue Eng* 2021; 12: 20417314211021679.
40. Yang T, Zhao F, Zhou L, et al. Therapeutic potential of adipose-derived mesenchymal stem cell exosomes in tissue-engineered bladders. *J Tissue Eng* 2021; 12: 20417314211001545.
41. de Abreu RC, Fernandes H, da Costa Martins PA, et al. Native and bioengineered extracellular vesicles for cardiovascular therapeutics. *Nat Rev Cardiol* 2020; 17: 685–697.
42. Yea J-H, Yoon YM, Lee JH, et al. Exosomes isolated from melatonin-stimulated mesenchymal stem cells improve kidney function by regulating inflammation and fibrosis in a chronic kidney disease mouse model. *J Tissue Eng* 2021; 12: 20417314211059624.
43. Huang C-C, Narayanan R, Alapati S, et al. Exosomes as biomimetic tools for stem cell differentiation: applications in dental pulp tissue regeneration. *Biomaterials* 2016; 111: 103–115.
44. Hu X, Zhong Y, Kong Y, et al. Lineage-specific exosomes promote the odontogenic differentiation of human dental pulp stem cells (DPSCs) through TGFβ1/smads signaling pathway via transfer of microRNAs. *Stem Cell Res Ther* 2019; 10: 170.
45. Zhuang X, Ji L, Jiang H, et al. Exosomes derived from stem cells from the apical papilla promote dentine-pulp complex regeneration by inducing specific dentinogenesis. *Stem Cells Int* 2020; 2020: 5816723.
46. Zhang S, Yang Y, Jia S, et al. Exosome-like vesicles derived from Hertwig's epithelial root sheath cells promote the regeneration of dentin-pulp tissue. *Theranostics* 2020; 10: 5914–5931.
47. Wang D, Lyu Y, Yang Y, et al. Schwann cell-derived EVs facilitate dental pulp regeneration through endogenous stem cell recruitment via SDF-1/CXCR4 axis. *Acta Biomater* 2022; 140: 610–624.
48. Wen B, Huang Y, Qiu T, et al. Reparative dentin formation by dentin matrix proteins and small extracellular vesicles. *J Endod* 2021; 47: 253–262.
49. Swanson WB, Gong T, Zhang Z, et al. Controlled release of odontogenic exosomes from a biodegradable vehicle mediates dentinogenesis as a novel biomimetic pulp capping therapy. *J Control Release* 2020; 324: 679–694.
50. Wang J and Feng JQ. Signaling pathways critical for tooth root formation. *J Dent Res* 2017; 96: 1221–1228.

51. Lee D-S, Park J-T, Kim H-M, et al. Nuclear Factor I-C is essential for odontogenic cell proliferation and odontoblast differentiation during tooth root development. *J Biol Chem* 2009; 284: 17293–17303.
52. Roh SY and Park J-C. The role of nuclear factor I-C in tooth and bone development. *J Korean Assoc Oral Maxillofac Surg* 2017; 43: 63–69.
53. Gao S, Zhao Y-M and Ge LH. Nuclear factor I-C expression pattern in developing teeth and its important role in odontogenic differentiation of human molar stem cells from the apical papilla. *Eur J Oral Sci* 2014; 122: 382–390.
54. Zhang J, Wang Z, Jiang Y, et al. Nuclear Factor I-C promotes proliferation and differentiation of apical papilla-derived human stem cells in vitro. *Exp Cell Res* 2015; 332: 259–266.
55. He W, Zhang J, Niu Z, et al. Regulatory interplay between NFIC and TGF-β1 in apical papilla-derived stem cells. *J Dent Res* 2014; 93: 496–501.
56. Zhang J, Zhang Y, Lv H, et al. Human stem cells from the apical papilla response to bacterial lipopolysaccharide exposure and anti-inflammatory effects of nuclear factor I C. *J Endod* 2013; 39: 1416–1422.
57. Sun J, Shen H, Shao L, et al. HIF-1α overexpression in mesenchymal stem cell-derived exosomes mediates cardioprotection in myocardial infarction by enhanced angiogenesis. *Stem Cell Res Ther* 2020; 11: 373.
58. Li X, Xie X, Lian W, et al. Exosomes from adipose-derived stem cells overexpressing Nrf2 accelerate cutaneous wound healing by promoting vascularization in a diabetic foot ulcer rat model. *Exp Mol Med* 2018; 50: 29.
59. de Camargo LCB, Guaddachi F, Bergerat D, et al. Extracellular vesicles produced by NFAT3-expressing cells hinder tumor growth and metastatic dissemination. *Sci Rep* 2020; 10: 8964.
60. Elsharkasy OM, Nordin JZ, Hagey DW, et al. Extracellular vesicles as drug delivery systems: Why and how? *Adv Drug Deliv Rev* 2020; 159: 332–343.